FISSION-PRODUCT RELEASE MODELLING IN THE ASTEC INTEGRAL CODE: THE STATUS OF THE ELSA MODULE

W. PLUMECOCQ, M. P. KISSANE, H. MANENC and P. GIORDANO

Institut de Radioprotection et de Sûreté Nucléaire, Département de Recherches en Sécurité,
B.P. 3, 13115 Saint Paul-Lez-Durance Cedex, France.

ABSTRACT

Safety assessment of water-cooled nuclear reactors encompasses potential severe accidents where, in particular, the release of fission products (FPs) and actinides into the reactor coolant system (RCS) is evaluated. The ELSA module is used in the ASTEC integral code to model all releases into the RCS. A wide variety of experiments is used for validation: small-scale CRL, ORNL and VERCORS tests; large-scale Phébus-FP tests; etc. Being a tool that covers intact fuel and degraded states, ELSA is being improved maximizing the use of information from degradation modelling. Short-term improvements will include some treatment of initial FP release due to intergranular inventories and implementing models for release of additional structural materials (Sn, Fe, etc.).

Keywords : severe accidents, safety, analysis, fission product, release, ASTEC.

1. INTRODUCTION

Fission-product (FP) release during a severe reactor accident could result in considerable discharges of radioactivity to the environment if the containment building is deficient. Such an accident involves coolant loss from the reactor coolant system (RCS, or PHTS in the CANDU community) leading to core overheating with partial or total liquefaction and release of FPs, actinides and structural materials. The releases from intact fuel, liquefying fuel, fuel debris, light-water reactor (LWR) control rods and a molten pool (see the general configuration depicted in Figure 1) are modelled in the ELSA v2.1 module. ELSA v2.1 is coupled to the core degradation module DIVA of the ASTEC V1 integral code [1].

All models employ a semi-empirical approach where ELSA v2.1 deals with 42 FPs, 5 actinides and 5 structural materials from LWRs. For solid fuel (intact or debris), FPs and actinides are divided into three empirically-observed, behaviour-dependent categories: volatile, semi-volatile or non-volatile as summarized in Table 1. This modelling only deals with the principal mechanism governing the release, i.e. the dominant limiting phenomenon, in each of these categories.

The modelling of the code is described below along with examples of validation studies where a wide variety of experiments is used including advanced degradation states such as in the large-scale Phébus-FP tests [2]. An indication is also given of future directions in terms of improvement and completion of the modelling.

2. VOLATILE FISSION-PRODUCT RELEASE FROM SOLID FUEL

The release rate of volatile FPs depends largely on the process of solid-state diffusion out of UO_2 fuel grains. In ELSA, the grains are assumed to be spherical and a grain size distribution is used to model the pellet. In addition, grain boundaries are assumed to be open rendering the resistance of this step in the release process unimportant. In other words, the rate-limiting step is diffusion out of the grains and all other effects are neglected. In particular, some volatile FPs can have significant pre-transient, intergranular inventories (i.e. a non-negligible fraction that has diffused out of the grains during normal reactor operation). The approximation of neglecting such inventories is most significant with respect to the fission gases but these are not of primary concern in the severe-accident context. Furthermore, the approach is based on tuning the effective diffusion coefficient used in the model on analytical, bare-fuel tests: this semi-empiricism mitigates to some extent the neglect of secondary effects. Nevertheless, the intergranular-inventory aspect probably requires review with the advent of increasing fuel burn-ups. Lastly, a final simplification is made by using a single value for the diffusion coefficient for all the volatile FPs; this value varies as a function of temperature and fuel oxidation (i.e., deviation from stoichiometry).

The instantaneous fractional release rate, τ, is obtained from the calculation of the release rate from a given grain in each size class and integrating all contributions over the distribution function:

$$\tau(t,x) = \frac{1}{m(t)}\frac{dm(t,x)}{dt} = \frac{V}{m(t)}\int_{r=0}^{\infty} \tau(r,t,x)\, m(r,t)\, f(r)\, dr$$

where V is the volume of the fuel component, $m(r,t)$ the current mass of a FP species in class r at time t, $f(r)$ the fraction of fuel grains with radius r assuming a log-normal function and x the stoichiometric deviation. The release rate of species from a given (spherical) fuel grain of radius r is obtained from the Booth formulation [3] by solving Fick's law. At time t_i we have:

$$\tau(r,t_i,x) = \frac{\pi^2 D_{i,i-1}}{r^2} \quad \text{if} \quad \frac{\pi^2 D\times t_i}{r^2} > 1$$

$$\tau(r,t_i,x) = \frac{3D_{i,i-1}}{r^2}\times\left(\frac{1}{\sqrt{\frac{\pi D\times t_i}{r^2}}} - 1\right)\times\frac{1}{\left(6\times\sqrt{\frac{D\times t_i}{\pi r^2}} - \frac{3D\times t_i}{r^2} - 1\right)} \quad \text{if} \quad \frac{\pi^2 D\times t_i}{r^2} \leq 1$$

where the diffusion coefficient over the period $(t_{i-1}, t_i]$ has been assumed constant. The diffusion coefficient D is given by:

$$\frac{\mathrm{D}\times \mathrm{t}_\mathrm{n}}{\mathrm{r}^2} = \frac{\sum_{\mathrm{i}=0}^{\mathrm{n}} \mathrm{D}_{\mathrm{i,i-1}}\times(\mathrm{t}_\mathrm{i} - \mathrm{t}_{\mathrm{i-1}})}{\mathrm{r}^2}$$

where $D_{i,i-1}$ is a function of temperature and stoichiometric deviation. This deviation, x, is described in ELSA as an oxygen exchange at the surface of the fuel [4]:

$$\frac{dx}{dt}=\alpha\left[x_{eq}(t)-x(t)\right]\frac{S_{eff}}{V}$$

where α is a function of temperature and has been experimentally determined between 1073K and 1873K for unirradiated fuel [5], x_{eq} is the equilibrium stoichiometric deviation with respect to the bulk oxygen potential and S_{eff}/V is the effective surface-to-volume ratio of the fuel where the surface area is that accessible to the bulk atmosphere. Hence, S_{eff} is the simple geometrical area multiplied by two correction factors, one increasing the area due to surface roughness and microcracking of the fuel and the other reducing the area accounting for the presence of cladding. This latter value is zero before the cladding reaches a state of almost complete oxidation.

During accident progression, UO_2 can liquefy due to eutectic formation with Zr or other materials. In this case, based on results observed in the VERCORS HT3 test [7] as well as in VEGA3 [6], 100 % of the remaining volatile FPs are released instantaneously from the liquid fraction. Such an approach also gives good results when compared with release rates measured in Phébus FP tests [8] – see below, this section.

The release of volatile FPs from debris beds is based on the same approach as used for intact fuel. The only difference concerns the definition of the average effective ratio S_{eff}/V used in the calculation of the stoichiometric deviation. The average geometrical ratio S^*/V^* is given by:

$$\frac{S^*}{V^*}=\frac{\sum_{i=1}^{n_{classes}} S(i)\times n_{part}(i)}{\sum_{i=1}^{n_{classes}} V(i)\times n_{part}(i)}=\frac{\sum_{i=1}^{n_{classes}} r^2(i)\times n_{part}(i)}{\sum_{i=1}^{n_{classes}} \frac{r^3(i)\times n_{part}(i)}{3}}$$

where $n_{classes}$ is the number of debris size classes, n_{part} the number of debris in a given class and r the radius of the debris classes. The correction factor for surface roughness and cracking, defined for release from intact fuel, is also applied to this average geometrical ratio to obtain the average effective ratio S_{eff}/V.

Figures 2 to 4 show examples of the release of volatile FPs predicted by ELSA compared to experimental data. The first example is the AECL test UCE9-5 which had an argon phase followed by a steam-argon phase while the fuel sample was held at nearly 1500K [9]. Agreement is seen to be quite reasonable with the effect of accelerated release due to fuel oxidation clearly reproduced. This agreement can be improved if it is recalled that the Ar used contained a non-negligible oxygen fraction which has not been accounted for here. The initial difference may also be related to the faster release in the test of a significant intergranular inventory. The second case shown is VERCORS 3, a test in a very steam-rich atmosphere with a maximum fuel temperature reaching 2200K [10]. It is seen that the agreement is excellent. For the Phébus FPT1 test [8], Figure 4, results are in good agreement except for Sb implying that the interaction with fuel cladding may not be satisfactory modelled (though agreement with results of analytical tests is quite reasonable). Half of the volatile FP inventory is released during the oxidation phase occurring at 11000 s. After 15000 s, the renewed heat up by the increasing bundle power leads to an enhancement of the volatile FP release due to the effect of liquefaction.

3. SEMI-VOLATILE FISSION PRODUCT RELEASE FROM SOLID FUEL

Semi-volatile FPs are thought to diffuse to grain boundaries at approximately the same rate as the volatile FPs but are released from the fuel at lower rates. A rate-limiting process at the grain boundary or from a phase or phases precipitated between the grains (e.g. Ru) is therefore indicated. In ELSA the release into the open fuel porosities of intact fuel and debris beds and then into the bulk atmosphere is assumed to be governed by evaporation and mass-transfer processes. The release rate of a semi-volatile species is given by:

$$\frac{dm_i}{dt} = \beta_i \, S \frac{P_i}{P_t} \rho_t$$

where S is the exchange surface area, β_i and P_i are, respectively, the mass transfer coefficient and the effective partial pressure of FP i in the gas at the evaporating surface in the fuel grain, P_t and ρ_t are, respectively, the total pressure of the gas and the molar concentration of gas in the bulk. Note that the pressure of a species i in the bulk gas of the porosities has been assumed negligible compared to the pressure of that species at the evaporating surface.

Simplified chemistry is used in the calculation of the effective partial pressures P_i. The method consists, for each element, of the prior identification of temperature-dependent correlations that give the best fit to thermodynamic-equilibrium calculations taking account of ambient gas conditions in analytical tests. It should be understood that the semi-empiricism of the approach means that no explicit knowledge of the various constants that arise (parameters such as β_i) is necessary since these comprise a single, compound constant that is determined empirically.

Concerning release from fuel debris, the approach is unchanged.

Strictly, the release of some semi-volatile FPs could depend on the diffusion through fuel grains and evaporation into pellet pores. Given the neglect of the diffusion step in the current modelling, a safeguard is implemented to prevent (as has been found on rare occasions) higher release of a semi-volatile FP compared to that of volatile FPs. Thus, a limitation on the release of semi-volatile FPs is applied such that the instantaneous fractional release rate of semi-volatile FPs cannot exceed that of volatile FPs except in the case where the total release of volatile FPs has been reached.

Figures 6 and 7 show examples of the results of this modelling for barium and molybdenum compared to the VERCORS tests [10]. Similar results have also been found for the ORNL HI/VI tests. It is seen that agreement is somewhat variable being often acceptable but occasionally unsatisfactory, particularly for Mo. This is thought to be due to incomplete understanding of the chemistry where the evaporating species used is not always appropriate (see §7).

4. LOW-VOLATILE FISSION-PRODUCT RELEASE FROM SOLID FUEL

Since low-volatility FPs do not diffuse significantly inside the fuel matrix, the release of these FPs from intact fuels as well as debris beds is assumed to be governed by the volatilization of UO_2. The fractional release is assumed to be equal to that of the volatilized fuel fraction. While this approach may be conservative for some FPs such as Zr, it is considered acceptable in the safety context that it provides a lower-limit release for all nuclides.

UO_2 volatilization is treated as the vaporization of UO_3 from the exposed fuel surface. UO_3 vapour can form in equilibrium with hyperstoichiometric UO_{2+x} fuel. The rate of volatilization is then proportional to the equilibrium UO_3 vapour pressure, directly related to the oxygen partial pressure of the atmosphere. The UO_3 vapour pressure in the gas bulk is assumed to be negligible. The approach used to model volatilization of UO_2 is, thus, similar to that of the release of semi-volatile FPs (though the evaporating surface is different) applying a mass-transfer limitation. Firstly, the correlation for the partial pressure of UO_3 is (Alexander's basic equations following the VICTORIA code [11]):

$$P_{UO_3} = 566.43 \exp\left(\frac{-\Delta G}{RT}\right) \times P_{O_2}^{\;0.45}$$

with ΔG = 250000- 83.3 T, T in Kelvin and P_{O2} is the oxygen partial pressure of the bulk atmosphere. Then the rate of U (as UO_3) mass loss is given by:

$$\frac{dm_{UO3}}{dt} = \beta_{UO3}\, S_{\text{eff}}\, \frac{P_{UO3}}{P_t}\, \rho_{\text{t}}$$

where S_{eff} is the effective fuel exchange area and the mass transfer coefficient, β_{UO3}, has been fitted to bare-fuel tests [5,12]. The multiplicative factors accounting for pellet roughness and cracking and the presence of cladding in the oxidation calculation for volatile FP release are included in S_{eff} here.

Comparison with analytical data from the FPRMP project of the E.U. 4th Framework Programme has shown that the model performs satisfactorily but that taking account of surface-reaction kinetics could improve the comparison [13] (i.e., the P_{UO3} does not instantaneously reach its equilibrium value at the pellet surface). Compared to results from the Phébus FPT1 test, good agreement is also found.

5. CONTROL-ROD RELEASES

Release concerns silver, indium and cadmium and/or boron and carbon depending on the type of rod, Ag-In-Cd alloy or B_4C. The model for boron carbide is a simple loss-through-oxidation correlation [14]. For Ag-In-Cd rods, due to its high volatility, Cd will be released in a burst upon rupture of the rod where the amount, in the empirical model used here, depends on gas conditions. In oxidizing conditions, Cd is assumed to be completely released from the liquid alloy contrary to the case of a reducing atmosphere where release of Cd is limited to 10%. Release of Ag, In and any remaining Cd will occur during the candling of the alloy after relocation of cladding. In the model of Ag-In-Cd volatilization during candling, there is no consideration of chemistry due to the bulk atmosphere. The released fraction is given by:

$$\tau = \left[1 - \exp(-\alpha_i \Delta t)\right]$$

where α_i is a function of total pressure, temperature and activation energy. The same correlations are applied for the release of Ag-In-Cd from the free surface of liquid alloy.

An example of the control-rod releases predicted by ELSA is shown for the Phébus FPT1 test, Figure 5. Release starts at burst occurrence with the release of 72 % of the Cd. Due to the early relocation of the absorber rod materials to the lower bundle, where the temperatures remained low, the release of Ag occurring during the candling remains low compared to experimental data (4 % of the initial inventory against ≈15 % in the experiment). Modelling improvements are in progress taking, most notably, better account of the geometry of the evaporating surface.

6. RELEASE FROM IN-VESSEL MOLTEN POOLS

The basis of the model is that, given the high-temperature conditions, chemical equilibrium can be assumed in the magma and that mass transfer limits evaporation from the free surface of the liquid phase. In addition, the molten pool is axially (vertically) and radially discretized using a fixed grid but there is no attempt to model correctly the physics of diffusion and convection phenomena between pool nodes. The approximation is, instead, to assume rapid homogenization of the pool. Hence, the transport model between pool nodes is based on diffusion where a single, temperature-independent diffusion coefficient with a very large value is applied to the whole magma, i.e., all species diffuse rapidly and at the same rate.

Central to the modelling is calculation of the vapour pressures of the elements at the surface of the molten pool. The vapour-pressure calculation requires comprehensive treatment of chemistry where the equilibrium assumption allows resolution by minimization of the Gibbs free energy of the system. The elements considered in the molten pool database are given in Table 2 (note that elements from concrete are included since the same database will be used by an ex-vessel model). The need to include an element in the pool was not determined solely by the radiotoxicity of its radioisotopes but also depended on the importance of its contribution to decay heating of the pool and/or its propensity to react with important elements. Generally, an ideal-solution approximation is used since data on non-ideal behaviour are largely lacking.

The evaporative rate of mass loss for a species is given by:

$$\frac{dm_i}{dt} = \beta_i S \frac{P_i M_i}{RT}$$

P_i and T are respectively the saturated partial pressure of species i and gas temperature at the pool surface, M_i the molar mass of species i, R the ideal gas constant, S the free surface area of the pool and β_i the mass transfer coefficient for species i. The β_i are based on the commonly-used Chapman and Enskog approach [15] requiring definition of collision diameters and Lennard-Jones potentials for each species. Correlations for mass transfer are taken from [16] with different expressions depending on whether convection is forced or natural and laminar or turbulent; a quadratic summation of the expressions is used for mixed convection.

The first application of the ELSA v2.1 code to the release of FPs from molten pools has been performed on two oxidic-melt experiments and a metallic-melt test from the LPP project of the E.U. 5th Framework Programme[1]. The particular interest of applying the ELSA code to these experiments was to test the purely evaporation-based model given that in-vessel conditions involve only steam-hydrogen atmospheres and, very probably, little if any sparging due to highly volatile components (the mixing of significant amounts of volatile species in such a pool to achieve sparging would appear precluded by their prior evaporation). The exercise showed that development effort will have to focus on the gas-phase chemistry to take account of the formation of gas-phase species other than those evaporating from the pool (e.g., UO_3 cannot form when only condensed phases are considered).

7. CONCLUSIONS

An overview of the physical models of the ELSA v2.1 code implemented in ASTEC v1 has been presented with some example calculations.

With respect to solid fuel, calculation of the release of volatile FPs is seen to be satisfactory though some improvement in release rates would be possible by taking account of intergranular inventories: these can lead in analytical tests to significant early release which is underestimated by ELSA. However, the importance of this has to be assessed in terms of other necessary improvements and the apparent insignificant incidence in large-scale tests such as Phébus FPT1 (though higher burn-ups need to be investigated). Regarding semi-volatile and low-volatile FP release, this can be strongly dependent on the chemistry taking place in the fuel. A semi-empirical approach with simple correlations, derived from thermodynamic equilibrium calculations, is used with tuning on experiments where the great majority of these have been performed in reactor-representative conditions. Nevertheless, the semi-volatile correlations will be reviewed based on more exhaustive exploration of the impact of the bulk atmosphere and in the light of work on interpretation of fuel chemistry using the MFPR code [17]. Lastly, the urania volatilization model used for all other releases may require addition of a second limiting step due to surface reaction kinetics. Alternatively, the oxidation model may require review (if the fuel over-oxidizes, this would also explain higher volatilization).

The in-vessel molten pool model is operational in ELSA v2.1 but data are lacking concerning its validation. Nevertheless, initial calculations indicate in particular that gas-phase chemistry cannot be ignored (rather than just dealing with chemistry in the pool for the evaporating species).

Additional models planned include implementing models for further structural materials (e.g. Zr, Sn, Ni, Fe, Cr). The case of an ex-vessel pool will also be dealt with based on already-prepared initial specifications and progress with modelling molten-core-concrete interactions in the ASTEC context. The longer term will concern generalized use of Material Data Bank

---

[1] These data are unpublished and proprietary; general details can be found in proceedings of recent (2002, 2003) FISA meetings organized by the European Commission for which EUR references do not yet exist.

(MDB), an IRSN tool used for chemical-equilibrium calculations, currently limited to the molten pool.

In conclusion, ELSA, now a robust and relatively mature tool, provides a sound basis for completing modelling of the relevant phenomenology and already comprises a suitable tool for prediction of FP release in many circumstances with a reasonable level of accuracy and an acceptable calculation time.

8. ACKNOWLEDGMENTS

The authors acknowledge the following contributions to development of ELSA v2.1: M. Notley (under contract to IRSN) on all aspects of release from solid fuel; R. Dubourg (IRSN) and T. Haste (SercoAssurance, under contract to IRSN) on release from SIC control rods; P. Mason (AEA Technology, under contract to IRSN) on molten-pool modelling and F. Jacq (IRSN) concerning the MDB solver.

9. REFERENCES

1. Van Dorsselaere, J.P., Jacq, F., Allelein, H.J. and Schwinges, B., "ASTEC code status and applications", US NRC CSARP meeting, Bethesda, USA, 5-7 May 2003 (2003).
2. Schwarz, M., Hache, G. and Von der Hardt, P., "PHEBUS FP: a severe accident research programme for current and advanced light-water reactors", Nucl. Eng. Des., 187, 47-69 (1999).
3. Booth, A.H., "A suggested method for calculating the diffusion of radioactive rare gas FPs from UO2 fuel elements and a discussion of proposed in-reactor experiments that may be used to test its validity", Atomic Energy of Canada Limited Report, AECL-700 (1957).
4. Lewis, B.J., Cox, D.S. and Iglesias, F.C., "A kinetic model for fission-product release and fuel oxidation behaviour for Zircaloy-clad fuel elements under reactor accident conditions", J. Nucl. Mat. 00710 (1993).
5. Cox, D.S. *et al.*, "Oxidation of UO_2 in air and steam with relevance to fission product releases", International Conference on CANDU fuel, Chalk River, Canada, Oct. 1986 ISBN 0-919784-13-5 (1986).
6. Kudo, T., "Effect of temperature and atmosphere on release of nuclides including short-life FPs – results of recent VEGA-3 through -5 tests", Proc. Fuel Safety Research Specialists' Meeting, March 2002, JAERI-Conf 2002-009 (2002).
7. Pontillon, Y., Ducros, G., Malgouyres, P.P., Fiche, C., Kissane, M., Boulaud, D. and Evrard, J.M., "Fission-product release and transport in severe-accident conditions: comparison between VERCORS HT1/HT2/HT3 experiments concerning UO_2 fuel in reducing and oxidizing conditions, with and without control rod components", US NRC CSARP meeting, Bethesda, USA, 5-7 May 2003 (2003).
8. Clément, B. and Haste T., "Comparison report on International Standard Problem ISP-46 (Phébus FPT1)", IRSN Note Technique SEMAR 03/021 revision 3, July 2003 (also: E.U. 5th Framework document SAM-THENPHEBISP-D005; to be issued as an OECD/NEA report after review).
9. Lewis, B.J., Iglesias, F.C., Hunt, C.E.L. and Cox, D.S., "Release kinetics of volatile fission products under severe accident conditions", Nuclear Technology, vol. 99, p. 330-342, (1992).

10. Ducros, G., Malgouyres, P.P., Kissane, M., Boulaud, D. and Durin, M., "Fission product release under severe accident conditions: general presentation of the program and synthesis of VERCORS 1-6 results", Nucl. Eng. Des. 208, 191-203 (2001).
11. T.J. Heames, D.A. Williams *et al.*, "VICTORIA: a mechanistic model of radionuclide behavior in the reactor coolant system under severe accident conditions", NUREG/CR-5545, SAND90-0756, Rev.1 (1992).
12. Cox, D.S., Hunt, C.E.L., Liu, Z. *et al.*, "A model for the release of low-volatility fission products in oxidizing conditions", Atomic Energy of Canada Ltd. report AECL-10440, (1991).
13. European Commission, "Nuclear fission safety – progress report 1988", report EUR 19115/1 (1999).
14. Adroguer, B. *et al.*, "Core loss during a severe accident (COLOSS)", Nucl. Eng. Des. 221, 55-76 (2003)
15. Chapman, S. and Cowling, T.G., "Mathematical theory of non-uniform gases", 2nd edition, Cambridge University Press (1951).
16. "Verein Deutscher Ingenieure Waermeatlas", VDI-Verlag GmbH, Düssseldorf (1984) – *in German*.
17. Nicaise, G., *et al.*, "Analysis of accidental sequence tests and interpretation of fission product release: interdependence of Cs, Mo, and Ba release", these proceedings.

Table 1: solid-fuel FP and actinide release categories and limiting phenomena

class Ia volatile FPs	*Xe, Kr, I, Cs, Br, Rb, Cu, Ag*	atomic diffusion, UO_{2+x} effect included
class Ib volatile FPs	*Te, Se, Sb*	as above plus trapping by unoxidized Zrly
class II semi-volatiles	*Sr, Ba, Ru, Mo, La, Ce, Y, Eu*	simplified chemistry plus evaporation
class III non-volatiles	*Rh, Pd, Tc, Nb, Zr, Nd, Pm, Gd, Tb, Dy, Ho, Er, Tm, Yb, Pr, Sm, Zn, As, Cd, Sn, Ga, Ge, In, U, Np, Pu, Am, Cm*	volatilization of UO_3

Table 2 : elements considered in the molten-pool model
(in parentheses: elements that might usefully be included but are not yet)

control rods	Ag, In, Cd, B, C
alloys (cladding, steels, Inconels)	Zr, Sn, Fe, Cr (Ni)
concrete (for ex-vessel)	Si, Ca, Al, Mg, K, Na (Ti)
volatile fission products	Te (others released before pool)
semi/low-volatile fission products	Ba, Sr, Mo, Ru, La, Ce (Eu, Rh, Y, Nd, Pr)
actinides	Pu, U (Np)
non-prototypical elements (experiments)	W (Hf, Re, Ir, Ar)
gases	H, O (N)

Typical configuration

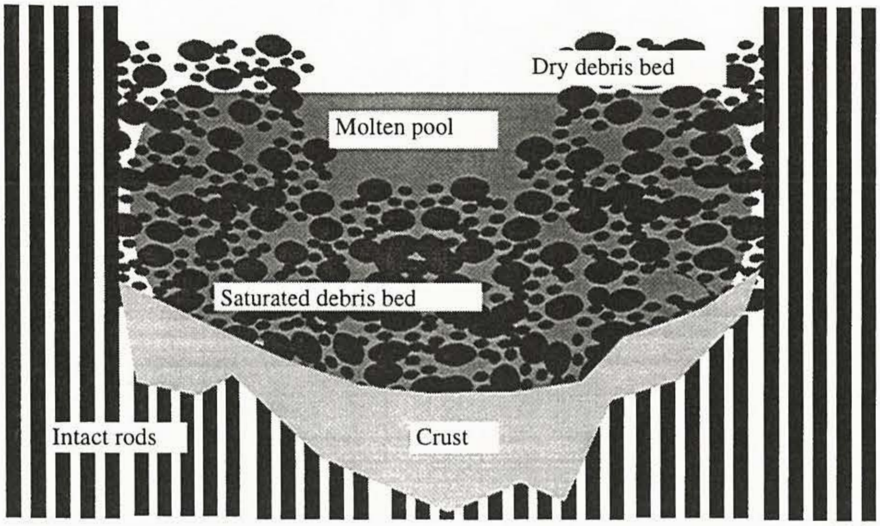

Figure 1: general, late-phase core configuration

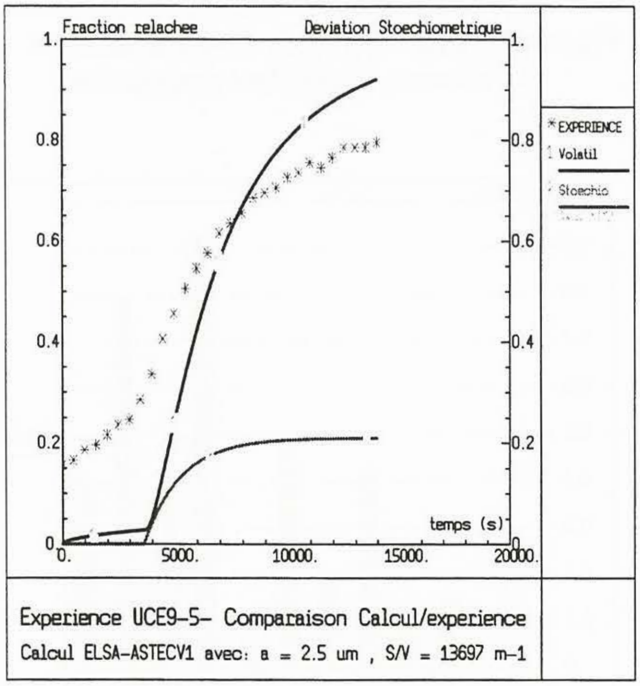

Figure 2 : UCE9-5, volatile FP release, ELSA/data comparison

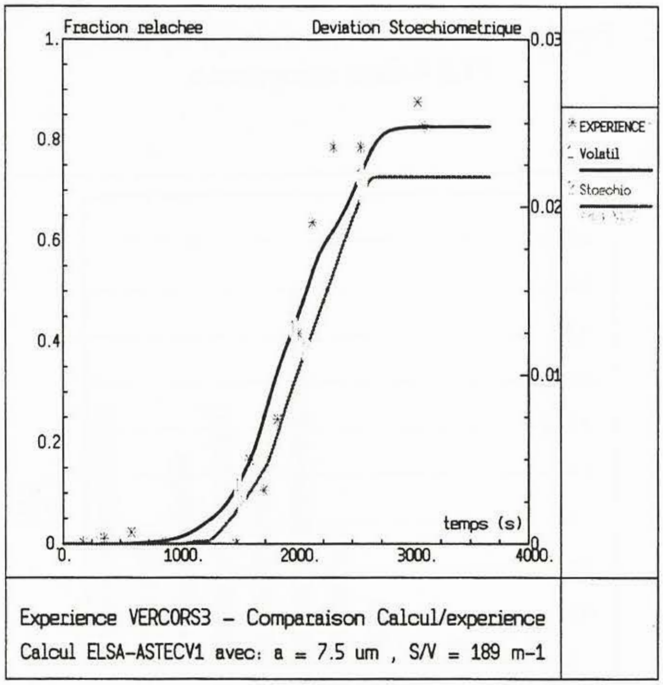

Figure 3: VERCORS 3, volatile FP release ELSA/data comparison

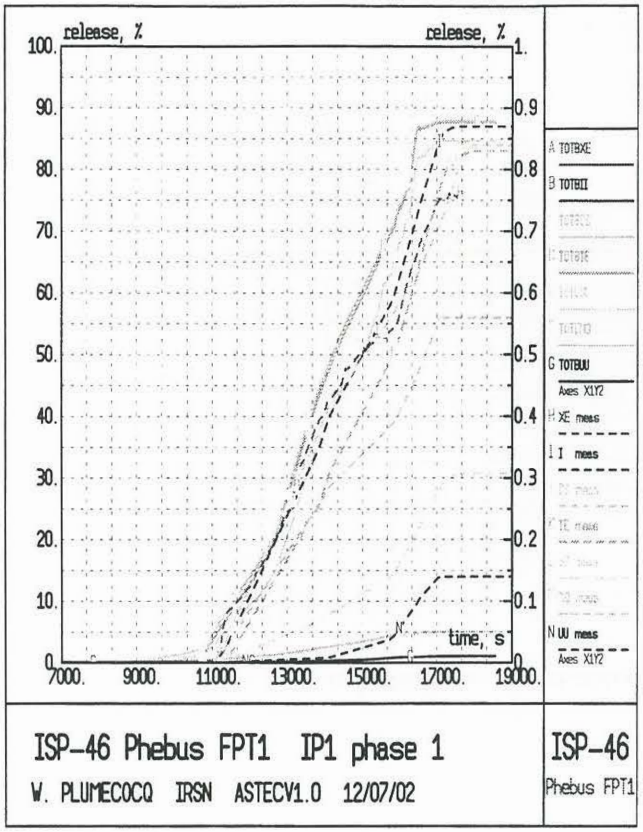

Figure 4: Phébus FPT1, volatile FP release, ELSA/data comparison

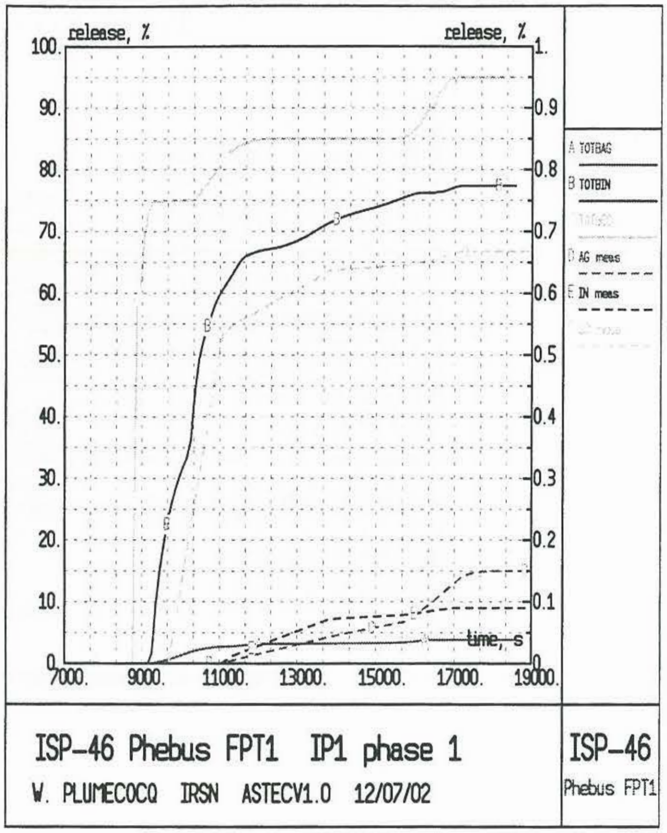

Figure 5: Phébus FPT1, Ag-In-Cd control rod releases, ELSA/data comparison

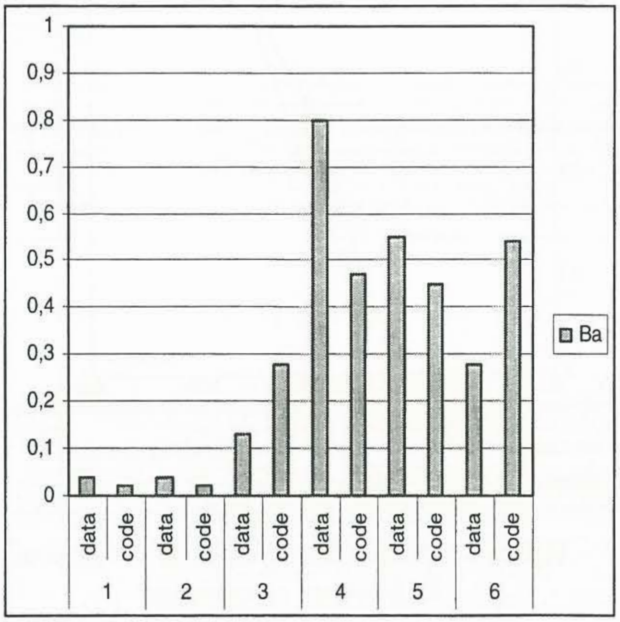

Figure 6: VERCORS 1 to 6, fractional release of Ba, ELSA/data comparison

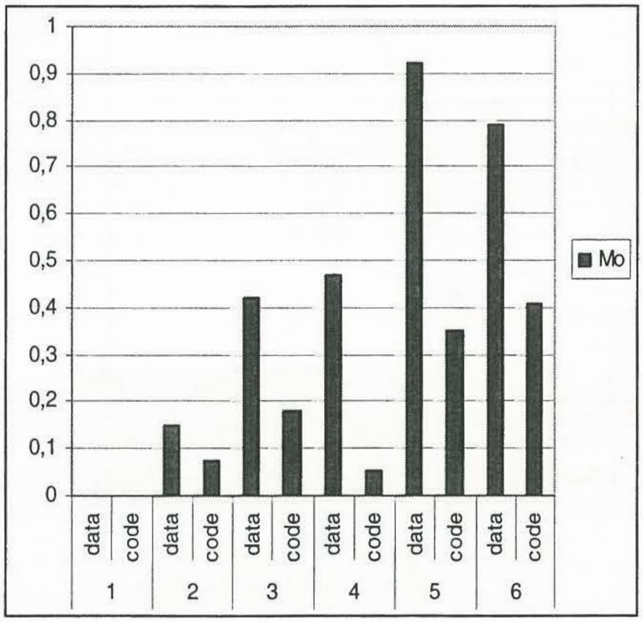

Figure 7: VERCORS 1 to 6, fractional release of Mo, ELSA/data comparison